Fiber Optic Current Transformers for Transformer Differential Protection during Inrush Current: a Field Study

Nikolay Ivanov
Skolkovo Institute of Science and Technology
Moscow, Russia
Nikolay.Ivanov@skoltech.ru

Petr Vorobev
Skolkovo Institute of Science and Technology
Moscow, Russia
P.Vorobev@skoltech.ru

Janusz Bialek
Skolkovo Institute of Science and Technology
Moscow, Russia
J.Bialek@skoltech.ru

Ruslan Kanafeev
JSC PROFOTECH
Moscow, Russia
Kanafeev@profotech.ru

Maxim Yanin
JSC PROFOTECH
Moscow, Russia
Yanin@profotech.ru

***Abstract*—Saturation of electromagnetic current transformers (EMCTs) due to inrush current during re-energizing of a power transformer may lead to misoperation of differential protection. Fiber optic current transformers (FOCTs) can offer a solution to this problem by providing an accurate replica of the primary current during inrush conditions as they are free from saturation. This paper focuses on comparing EMCTs and FOCTs measurements of inrush current based on data obtained during a field test at a 500 kV substation. Waveform and harmonic analysis of the signals captured by a digital fault recorder from EMCTs and FOCTs reveal a significant difference in their RMS and harmonic content, thus demonstrating the influence of the saturation of the EMCTs on the current measurements. We also show that compared to EMCT, FOCTs measurements allow for better identification of the inrush current by means of DC component analysis.**

***Index Terms*—inrush current, fiber optic current transformers (FOCTs), electro-magnetic current transformers (EMCTs), saturation, DC ratio blocking method**

I. Introduction

Nowadays, the power systems are under transformation, integrating advanced information and communication technologies, modern sensors, and increasingly smart devices that enhance overall grid reliability, stability, and security, thereby contributing to the transition towards Smart Grids [1]. Digitalization is one of the leading trends of the 21st century in many industries, and power systems are not an exception. The introduction of the so-called *digital substations* [2] is one of the steps in this transformation.

What makes an electrical substation a digital one? First of all, in digital substations, the interaction between secondary equipment underwent a change. Namely, the introduction of the process and station bus architecture with modern protocols as defined in the IEC 61850 standard allows additional flexibility for configuration and interoperability between different secondary equipment vendors [3]. Secondly, the adoption of non-conventional instrument transformers (NCITs) based on advanced techniques of current and voltage sensing (e.g., Rogowski coil, Pockels effect, and Faraday effect) brings substantial benefits. The ability of NCITs to produce outputs already in digital form enables the transition towards the digital substation at the process level, thus removing the need for copper wire links between a switch-yard and a control house. Fiber-optic current transformers (FOCTs), one of the most promising types of NCITs, are of particular interest since they provide higher quality current measurements than conventional electro-magnetic current transformers (EMCTs), which are known to suffer from saturation effects, especially at high current values [4], [5].

The active development of fiber optic technology for current measuring took place in the 1990s [6], [7], with the first commercially available FOCTs deployed at substations in the early 2000s [8], [9]. It was shown that FOCTs could be used in place of EMCTs as they meet the requirements for measurement standards for protection and metering purposes; hence they can be used with the existing relays and meters. Thus, multiple sources emphasize that FOCTs may bring possibilities to improve protective relaying performance in terms of speed, security, and dependability due to high accuracy, enhanced frequency response characteristics, and an absence of saturation impact on relays [2], [4], [10]. The characteristics and performance of FOCTs were extensively investigated both in lab conditions [11], [12] and in the field ones (at the actual electrical substations) [13]. It was shown that FOCTs are free from the saturation effect at high currents, typical for EMCTs, which makes them a well-reasoned choice for protection applications [14]. Thus, the excellent performance of FOCTs measuring fault currents was explicitly demonstrated [4].

Despite a number of already available studies on FOCTs,

978-1-6654-3597-0/21/$31.00 ©2021 IEEE

they are still an emerging technology, which requires additional research. Thus, there is a lack of systematic studies on the performance of FOCTs in specific applications that would thoroughly illustrate their numerous advantages over EMCTs. Likewise, the issue of adjusting the protection relays algorithms for operation with FOCTs instead of EMTCs is not well studied. In particular, the algorithms for transformer inrush current detection - an important practical issue - are not well covered. In the present work, based on the field data, we show that the usage of FOCTs can potentially enhance the sensitivity and security of transformer differential protection under inrush current as they are cable of providing a true replica of the primary current. We demonstrate that the better detection of the inrush current (compared to EMTCs) is possible by DC component analysis.

The rest part of the paper is organized in the following order. Section II includes information about fiber-optic sensing technology, inrush current phenomena and presents how differential protection tackles the inrush current. Section III presents the comparative analysis of EMCTs' and FOCTs' performance under inrush current, including short site description, waveform analysis, and harmonic spectrum analysis. Based on the differences in harmonic content, Section IV discusses the DC ratio blocking method. Conclusions and plans for future research are made in Section V.

II. Research Background

A. Fiber-optic Current Transformers

FOCTs belong to a family of NCITs. FOCTs exploit a non-electrical principle called the magneto-optical Faraday effect to measure currents, making them distinct from the EMCTs based on the electromagnetic induction principle. Following the Faraday effect, the circular birefringence arises in the optical medium under the external magnetic field. Therefore, the phase shift occurs between two circularly polarized light waves propagating through the medium near a conductor, as shown in 1. It is possible to determine the magnitude of the current by calculating this shift as the shift is proportional to the longitudinal component of the magnetic field generated by this current [15].

A typical FOCT consists of three main parts: (1) sensing head with fiber loops, (2) electronic process unit (EPU), and (3) an optic fiber cable linking them together as shown in 1. FOCTs are equally applicable for measurements of both AC and DC currents - another advantage over EMCTs. The number of fiber turns in the head is determined by the rated current. Overall, FOCTs provide high accuracy measurements over an extensive dynamic range under a wide temperature range. Due to immunity to saturation, FOCTs achieve high accuracy during transient events, and they are not affected by an effective load of the secondary equipment. Also, FOCTs themselves do not have any adverse effect on secondary networks due to their negligible capacity and inductance. It is possible to use the same fiber loop for revenue metering and protection purposes by setting the sampling rate in EPU. Moreover, it is possible to introduce several independent fiber loops, completely non-interacting with each other in one sensing head, to measure and transmit the same values of current through the main and backup channels. The characteristics of the FOCTs, such as frequency response, phase error, and phase displacements, were investigated in [11], [12].

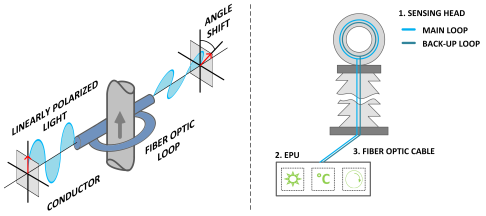

Fig. 1. Principal of FOCT and its main components

B. Inrush Current Phenomenon

The re-energizing of a power transformer is followed by the magnetizing inrush current. In many cases, it results in a state when a power transformer gets saturated. Inrush current is caused by a summation of a residual flux stored in a transformer core after switching it off and a newly generated flux when a power supply is restored. The transformer inrush current is rich in DC content and can occur in two forms: unipolar (asymmetrical) and bipolar (symmetrical). Voltage angle, magnitude, the polarity of residual flux at switching instant, and the total resistance of the primary winding are all factors that determine a character of a transient process. [5].

C. Inrush Current for Differential Protection

The increased magnitude of the inrush current usually does not directly threaten the power transformer's safety. The main concern with the inrush current is that it misleads the power transformer protection by appearing as a differential current for the corresponding relays [16], [17]. Such misrepresentation by power transformer protection might result in false relay triggering that eventually may lead to unwanted switching off of the power transformer, followed by more harmful consequences for the power system utilities. This fact creates a problem of distinguishing the true short-circuit currents caused by internal faults from magnetizing inrush currents occurring during a regular power transformer's re-energizing. The power transformer differential protection must be blocked and/or restrained during inrush conditions until the transient process dies away to prevent unwanted tripping. Different techniques were developed to restrain and/or block the differential relays.

The most common approach is to analyze the harmonic content of the current. The extraction of harmonics from the current can provide sufficient information that can be used to distinguish between internal faults and inrush conditions. Thereby, harmonic-based methods were used to develop different blocking and/or restraining principles. In particular, one of the main methods is based on the content of the 2-nd harmonic, which is typically substantial during the inrush current periods. The blocking threshold is usually set around $15-20\%$ from the fundamental harmonic value. However, it was shown that the

2-nd harmonic method could not guaranty absolute reliability because there are circumstances when its level can drop below the established threshold [16], thus preventing protection from blocking. Due to this reason, more complex approaches are being constantly proposed and developed, such as the principles based on even-harmonic restraint, fifth-harmonic blocking, DC ratio blocking [18], [19], wave-shape recognition principle based on the low currents intervals [20], and wavelet principle, etc. [21].

All the mentioned methods are very demanding on the quality of measurements so that the instruments transformers used can significantly influence the differential relays' ability to distinguish correctly between the inrush currents and internal faults. A very slowly decaying DC offset, typical for inrush current, can draw the EMCTs into the saturation or even into a more severe ultra saturation condition [16]. Saturated EMCTs introduce considerable distortions into the currents of the secondary circuit, and thus, it brings additional challenges for differential relays in distinguishing between internal faults and inrush currents. The adverse effects of the saturated current transformer on differential protection were described in [17]. Different approaches were developed to compensate for the saturation in EMCTs [22]–[24]. Unlike EMTCs, FOCTs do not suffer from the saturation effect, making it much easier to use any algorithms for inrush current detection. For this very reason, the analysis of FOCTs' and EMCTs' performance under inrush conditions is of particular interest since it compares two different principles of current measuring. The analysis can give a quantitative and qualitative assessment of the degree of distortions in current measurements imposed on the differential relays by saturated EMCTs.

III. Inrush Current Analysis

The data introduced in this section was obtained from a recently commissioned 500 kV digital substation "Tobol" located in Tyumen Region, Russia, and owned by the Federal Grid Company (Rosseti)[1]. The substation is a major part of a pilot project aimed at developing and field testing a measurement subsystem based on the IEC 61850 standard. Different vendors of power protection systems and revenue metering test their equipment and study possible compatibility issues under real conditions. One of the project's key objectives is the comparative analysis of the EMCTs' and FOCTs' performance under field test conditions.

A. Site and Experiment Description

The inrush current analysis is based on EMCTs' and FOCTs' measurements during a test re-energizing procedure of the 500 kV auto-transformer (AT) at a 50 Hz electrical system. A simplified electrical scheme is shown in Fig. 2, where two substations are linked with each other by a 500 kV line with a total length of 1.5 km. EMCTs and FOCTs are installed at the Substation 1. In Fig. 2, the blue circle with two arrows inside represents three-phase FOCTs, and the two orange circles represent three-phase EMCTs. A 250 MVA auto-transformer (AT) with the "star-delta" configuration, which was subject to re-energization, is installed at the Substation 2. Red arrows indicate the direction of the inrush current.

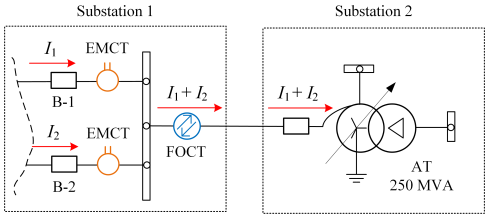

Fig. 2. Simplified single-line diagram.

The test procedure was performed as follows. First, the AT's load was switched off from the middle and low voltage sides. Then circuit breakers B-1 and B-2 at the Substation 1 were switched off to de-energize the transformer. Next, the AT was re-energized after several minutes.

The waveforms present in this analysis were captured by a digital fault recorder (DFR) installed at the Substation 1. The DFR simultaneously received analog signals from two EMCTs and digital signals from FOCTs. The DFR performed summation of two analog signals from currents I_1 and I_2 flowing through separate EMCTs to obtain the total inrush current measurement. The analog signals were digitized by a Merging unit. Digital measurements from EMCTs and FOCTs were transmitted as Sampled Values (SV80) according to the IEC 61850-9.2LE protocol. The DFR captured the first 5 seconds of the inrush current, which was then used in our analysis. We note, though, that the inrush current lasted significantly longer due to a high X/R ratio caused by the absence of the load.

B. Waveform Analysis

This subsection presents the waveform analysis of the inrush current measurements Fig. 3 shows the measurements of the inrush current obtained from EMCTs (orange) and FOCTs (blue) superimposed against each other. Phase A has a unipolar form of the inrush current, while phases B and C - bipolar forms.

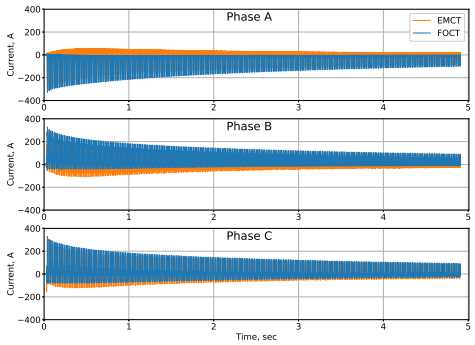

Fig. 3. The first 5 sec of the inrush current from EMCTs and FOCTs.

[1]Rosseti, Public Joint Stock Company, http://www.rosseti.ru/eng/

One can see in Fig. 4 that during the first cycle (first 20 ms), the difference between EMCTs and FOCTs measurements is negligible as the curves are completely overlapped. However, as the inrush current progresses, one can see the growing discrepancy between the measurements. The orange curve tends to move upward for phase A and downwards for phases B and C. The discrepancy between the orange and blue curves (measurements of EMTCs and FOCTs, respectively) achieves maximum during the first second and then gradually decays as the amplitude of the inrush current decreases. It can be concluded that this discrepancy results from the EMCTs saturation effect, which is more pronounced at the higher current values.

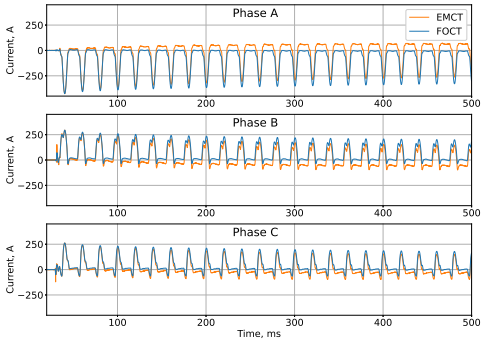

Fig. 4. First 25 cycles of inrush current from EMCTs and FOCTs.

Next, one can see that this growing discrepancy also results in a more significant difference between the measured current peak values. Namely, the current peak values measured by the EMCTs are lower than the corresponding values obtained from FOCTs. Likewise, the measured RMS current value is also affected. Fig. 5 shows that the measured current RMS is consistently lower for EMCTs compared to FOCT. The relative error can be as high as $15-20\%$ (black curves in Fig. 5).

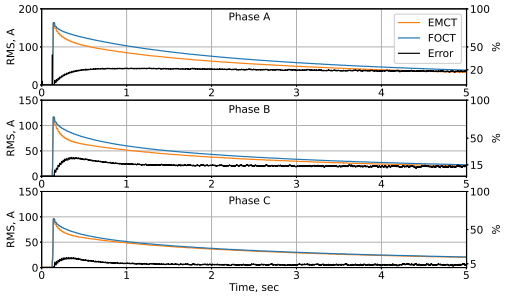

Fig. 5. Difference in RMS current between EMCTs and FOCTs including the relative errors at three phases.

C. Harmonic Spectrum Analysis

The analysis of the harmonic content of the measured inrush current for EMCTs and FOCTs is presented below. Fig. 6 presents the changes of DC, 1st, and 2nd harmonics (in absolute values) for EMCTs and FOCTs measurements at Phase A. One sees from Fig. 6, that the 1st and 2nd harmonics are the same for both EMCT and FOCT measurements, while the DC components are significantly different. One can see that for EMCTs, the magnitude of DC content fades away after around 0.6 sec. The DC component of the FOCT signal, in contrast to EMCTs, has a much slower decaying rate. We note that the harmonic behavior of the measurements obtained from phases B and C is similar to that of phase A.

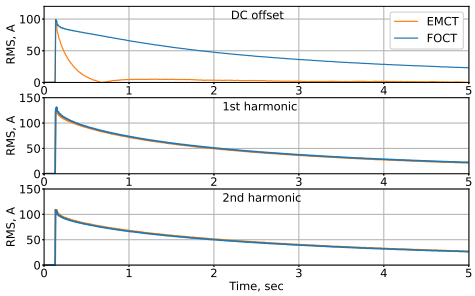

Fig. 6. Difference in DC offset, 1st and 2nd harmonics between EMCTs and FOCTs at phase A.

The Fig. 7 shows the change of the DC and the 2nd harmonic contents relative to the 1st - fundamental harmonic (in percent). The 2nd harmonic content is the same for both EMCTs and FOCTs. Again, a significant difference is present in the DC component. In the beginning, the levels of the DC components are the same for both signals. As the inrush current progresses, the DC content of the EMCTs signal decayed almost to zero after 0.6 s. On the contrary, the DC content of the FOCT signal gradually increases and eventually exceeds 100% relative to the fundamental.

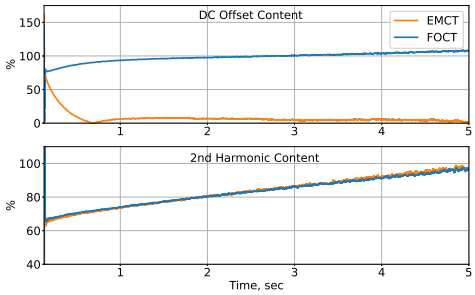

Fig. 7. Difference in content of DC offset and 2nd harmonic content relative to 1st harmonic at phase A.

Hence, the inability of EMCTs to represent the true level of the DC current component misleads the protection system about the real picture of the transient process. The fact that FOCTs can correctly measure the DC component can be used for refining and re-tuning the differential protection settings to increase the sensitivity of the inrush current detection algorithms. As an example, a blocking method using the DC component of inrush current is considered below.

IV. DC BLOCKING METHOD

The DC blocking method's idea proposed in [19] is to consider (Fig. 8) the areas under the positive (S^+) and negative

(S^-) values of the current measurement curve over one cycle, i.e., for S^+:

$$S^+ = |\sum_{k=1}^{N} i_k| \rightarrow (i_k > 0) \quad (1)$$

$$S^+ = 0 \rightarrow (i_k \leq 0) \quad (2)$$

Likewise, for S^-:

$$S^- = |\sum_{k=1}^{N} i_k| \rightarrow (i_k < 0) \quad (3)$$

$$S^- = 0 \rightarrow (i_k \geq 0) \quad (4)$$

where i_k represents the current samples, and N is the number of samples per cycle.

After S^+ and S^- are calculated, one finds their ratio by dividing the smaller value (min) by the bigger one (max). This gives the parameter called the DC-ratio (DCR) that can be between 0 and 1. By comparing the DCR value to a preset threshold $DCRF$, the differential relay blocking decision is made based on the following logic. The relay functions without blocking when $DCR > DCRF$. As soon as $DCR < DCRF$, the relay is blocked and stays blocked (relay does not react to the present differential current) while this inequality is met (Fig. 8) [25].

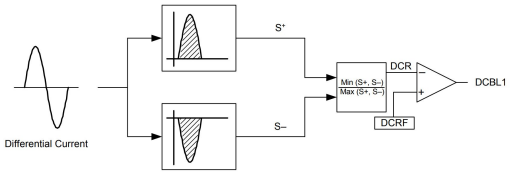

Fig. 8. DC blocking logic.

The DC blocking response almost exclusively depends on the DC component in the measurement of the differential current. Selecting a proper value for $DCRF$ means deciding on a compromise between security and relay response speed. A high value of $DCRF$ affords high security but is detrimental to the speed of response. Considering the difference of DC content for EMCTs and FOCTs measurements of inrush current, it is possible to show that the DC blocking method can be tuned more sensitive for FOCTs because $DCRF$ can take a significant lower value.

Fig. 9 shows two curves of an inrush current measurements in phase A for EMCTs and FOCTs for one cycle, corresponding to around 1 s time from the Fig.3. As was discussed earlier, the orange curve is shifted up because of the saturation effect in the EMCTs. Thus, the current measured by EMCTs oscillates between positive and negative values. Area calculation for the EMCT curve shows that the total positive area S^+_{EM} consists of two parts (S^+_{EM1} and S^+_{EM2} in Fig.9) with the areas of 0.1507 and 0.4286 respectively. Thus, the total positive area is 0.5793. The total negative area S^-_{EM} for EMCTs curve is 0.5127. By dividing the smaller value by the bigger one, the DCR_{EM} is found to be 0.88503. This value is relatively large and close to the case for a clear sinusoidal current for which $DCR = 1$. This means that for the EMTCs, the threshold $DCRF$ has to be rather large in order to provide the required security.

In contrast to EMCTs, the curve for FOCTs lies entirely in the negative part. Thus, the total positive area S^+_{FO} is zero, and the total negative area S^-_{FO} is 0.9681. Their division always gives $DCR_{FO} = 0$.

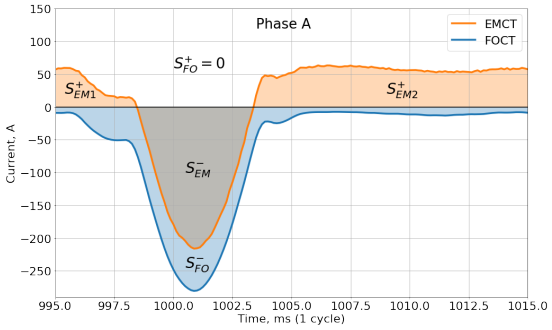

Fig. 9. Difference in areas for one cycle: $S^+_{EM1} = 0.1507$; $S^+_{EM2} = 0.4286$; $S^+_{EM} = 0.5793$; $S^-_{EM} = 0.5127$; $DCR_{EM} = 0.88503$; $S^+_{FO} = 0$; $S^-_{FO} = 0.9681$; $DCR_{FO} = 0$.

Fig. 10 shows the DCR-vales (as functions of time) for both EMTCs and FOCTS measurements in all three phases over the time period of 5 s (corresponding to current measurements from Fig.3). In the beginning, both DCR_{EM} and DCR_{FO} are zero due to zero transformer current. However, already after the first cycle of the inrush current DCR_{EM} and DCR_{FO} start to behave very differently. The DCR_{EM} increases rapidly during the first 0.6 sec (30 cycles) due to saturation. When EMCTs achieves the maximum level of saturation, the DCR_{EM} hits the maximum possible value of 1, and then stays close to it for the rest of the time interval (5s), indicating an apparent absence of the DC component (in accordance with Fig.6 and Fig.7). The DCR_{FO}, on the contrary, stays close to zero in phase A, and slowly grows to the values 0.1269 and 0.3501 in phases B and C, respectively. Table I shows the values of DCR for the first cycle and its mean values for the whole time interval in three phases. It can be seen that DCR_{FO} takes significantly smaller values than DCR_{EM}. Thereby, the observations presented in Fig. 10 and Table I show that the $DCRF$ for FOCTs can be set much lower to guaranty sufficient security and high sensitivity at the same time.

TABLE I
COMPARISON OF DCR.

	DCR_{EM}	DCR_{FO}	DCR_{EM}	DCR_{FO}
	1st cycle		*Mean value*	
Phase A	0.0806	0.0302	0.8749	0.0018
Phase B	0.0275	0.0173	0.8917	0.1077
Phase C	0.0872	0.0793	0.9001	0.3125

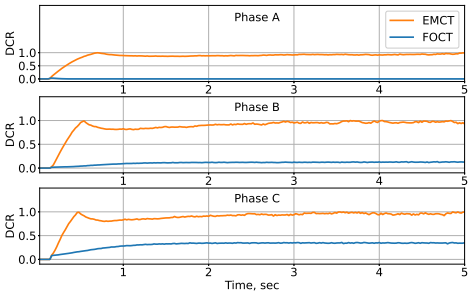

Fig. 10. Comparison of DCR_{EM} and DCR_{FO} during the inrush current.

V. Conclusions

This paper presented the comparative analysis of the inrush current measurements obtained from EMCTs and FOCTs during a 250 MVA auto-transformer re-energizing. Waveform analysis of both measurements showed a significant difference between them in all three phases. This difference is caused by the EMCTs' saturation effect that led to its current distortions compared to measurements from FOCTs, which were not subjected to saturation.

The distortions observed at the EMCTs measurements led to a decrease in the overall RMS values of current. The RMS values of the measured current at FOCTs are consistently higher (up to $15-20\%$) over the considered time period of 5s (Fig.5). Since the RMSs of the fundamental and the 2nd harmonic are the same for both EMCTs and FOCTs (Fig.6), thus the difference in RMS values is mainly caused by the different measurements of the DC component in the inrush current. Thus, the failure of the EMCTs to correctly measure the DC component of the current can be misleading for the protection system over the entire transient process. Finally, it was shown that the DC ratio blocking method in differential relays could potentially be tuned much more sensitive when FOCTs are used instead of EMCTs, thus, contributing to an overall increase in the security of transformer differential protection during inrush conditions.

Further research will focus on developing new methods for FOCTs data processing to increase the sensitivity of protection systems, including optimal threshold settings for inrush current detection. In addition, other FOCTs' applications will be explored, for instance, the protection of shunt. In addition, other FOCTs' applications, such as shunt protection, will be explored [26].

References

[1] M. Panteli and P. Mancarella, "The grid: Stronger, bigger, smarter?: Presenting a conceptual framework of power system resilience," *IEEE Power and Energy Magazine*, vol. 13, no. 3, pp. 58–66, 2015.

[2] R. Hunt, B. Flynn, and T. Smith, "The substation of the future: Moving toward a digital solution," *IEEE Power and Energy Magazine*, vol. 17, no. 4, pp. 47–55, 2019.

[3] F. Clavel, E. Savary, P. Angays, and A. Vieux-Melchior, "Integration of a new standard: A network simulator of iec 61850 architectures for electrical substations," *IEEE Industry Applications Magazine*, vol. 21, no. 1, pp. 41–48, 2014.

[4] R. E. Cosse, D. G. Dunn, and R. M. Spiewak, "Ct saturation calculations: Are they applicable in the modern world?—part i: The question," *IEEE Transactions on Industry Applications*, vol. 43, no. 2, pp. 444–452, 2007.

[5] A. Hargrave, M. J. Thompson, and B. Heilman, "Beyond the knee point: A practical guide to ct saturation," in *2018 71st Annual Conference for Protective Relay Engineers (CPRE)*. IEEE, 2018, pp. 1–23.

[6] T. Sawa, K. Kurosawa, T. Kaminishi, and T. Yokota, "Development of optical instrument transformers," *IEEE Transactions on Power Delivery*, vol. 5, no. 2, pp. 884–891, 1990.

[7] T. W. MacDougall, D. R. Lutz, and R. A. Wandmacher, "Development of a fiber optic current sensor for power systems," *IEEE transactions on power delivery*, vol. 7, no. 2, pp. 848–852, 1992.

[8] G. Sanders, J. Blake, A. Rose, F. Rahmatian, and C. Herdman, "Commercialization of fiber-optic current and voltage sensors at nxtphase," in *2002 15th Optical Fiber Sensors Conference Technical Digest. OFS 2002 (Cat. No. 02EX533)*. IEEE, 2002, pp. 31–34.

[9] F. Rahmatian and A. Ortega, "Applications of optical current and voltage sensors in high-voltage systems," in *2006 IEEE/PES Transmission & Distribution Conference and Exposition: Latin America*. IEEE, 2006, pp. 1–4.

[10] M. Kezunovic, L. Portillo, G. Karady, and S. Kucuksari, "Impact of optical instrument transformer characteristics on the performance of protective relays and power quality meters," *IEEE/PES Transmission Distribution Conference and Exposition*, pp. 1–7, 2006.

[11] S. Kucuksari and G. Karady, "Experimental comparison of conventional and optical current transformers," *IEEE Transactions on Power Delivery*, vol. 25, no. 4, pp. 2455–2463, 2010.

[12] ——, "Complete model development for an optical current transformer," *IEEE Transactions on Power Delivery*, vol. 27, no. 4, pp. 1755–1762, 2012.

[13] F. Rahmatian, "Optical instrument transformers," pp. 18–25, 2018.

[14] J. Hrabluik, "Optical current sensors eliminate ct saturation," in *2002 IEEE Power Engineering Society Winter Meeting. Conference Proceedings (Cat. No. 02CH37309)*, vol. 2. IEEE, 2002, pp. 1478–1481.

[15] Y. V. Przhiyalkovskiy, N. I. Starostin, V. P. Gubin, S. K. Morshnev, and A. I. Sazonov, "Fiber-optic sensor for detecting electric current pulses," in *Optical Sensors 2019*, vol. 11028. International Society for Optics and Photonics, 2019, p. 110280A.

[16] S. Hodder, B. Kasztenny, N. Fischer, and Y. Xia, "Low second-harmonic content in transformer inrush currents-analysis and practical solutions for protection security," in *2014 67th Annual Conference for Protective Relay Engineers*. IEEE, 2014, pp. 705–722.

[17] M. Stanbury and Z. Djekic, "The impact of current-transformer saturation on transformer differential protection," *IEEE Transactions on Power Delivery*, vol. 30, no. 3, pp. 1278–1287, 2014.

[18] R. Hamilton, "Analysis of transformer inrush current and comparison of harmonic restraint methods in transformer protection," *IEEE Transactions on Industry Applications*, vol. 49, no. 4, pp. 1890–1899, 2013.

[19] A. Guzman, H. Altuve, and D. Tziouvaras, "Power transformer protection improvements with numerical relays," *CIGRE Study Committee B5–Protection and Automation*, vol. 11, 2005.

[20] A. Guzman, S. Zocholl, G. Benmouyal, and H. J. Altuve, "A current-based solution for transformer differential protection. ii. relay description and evaluation," *IEEE Transactions on Power Delivery*, vol. 17, no. 4, pp. 886–893, 2002.

[21] J. Faiz and S. Lotfi-Fard, "A novel wavelet-based algorithm for discrimination of internal faults from magnetizing inrush currents in power transformers," *IEEE Transactions on Power Delivery*, vol. 21, no. 4, pp. 1989–1996, 2006.

[22] J. Pan, K. Vu, and Y. Hu, "An efficient compensation algorithm for current transformer saturation effects," *IEEE Transactions on Power delivery*, vol. 19, no. 4, pp. 1623–1628, 2004.

[23] Y. C. Kang, U. J. Lim, S. H. Kang, and P. A. Crossley, "Compensation of the distortion in the secondary current caused by saturation and remanence in a ct," *IEEE Transactions on Power Delivery*, vol. 19, no. 4, pp. 1642–1649, 2004.

[24] E. Hajipour, M. Vakilian, and M. Sanaye-Pasand, "Current-transformer saturation compensation for transformer differential relays," *IEEE Transactions on Power Delivery*, vol. 30, no. 5, pp. 2293–2302, 2015.

[25] J. H. Harlow, *Electric power transformer engineering*, 3rd ed. CRC press, 2012.

[26] F. K. Basha and M. Thompson, "Practical ehv reactor protection," in *2013 66th Annual Conference for Protective Relay Engineers*. IEEE, 2013, pp. 408–419.